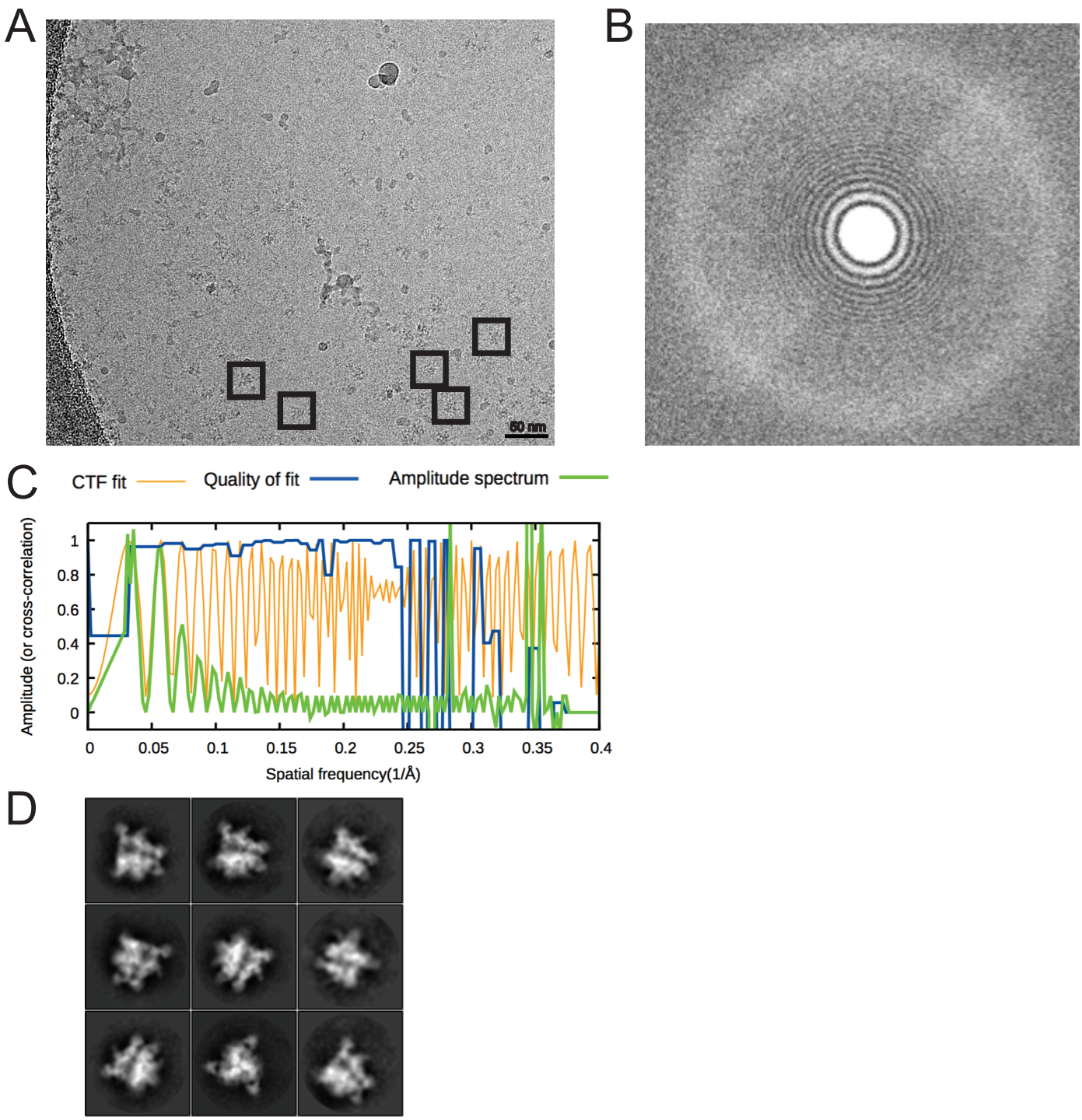

Fig. S1. 8.9 Å EM structure determination. (*A*) Image of the sample grid used for 8.9 Å reconstructions of the Env-sCD4-17b-8ANC complex. Examples of complex particles are boxed. The accumulated dose and defocus values were ~25 e-/Å^2 and ~2.2 µm underfocus. (*B*) Fourier transform of the micrograph in panel *A*. (*C*) CTF fitting of the left micrograph (generated using CTFFIND4) shows a good fit to 4.0 Å (*D*) Representative reference-free 2D class averages calculated by RELION.

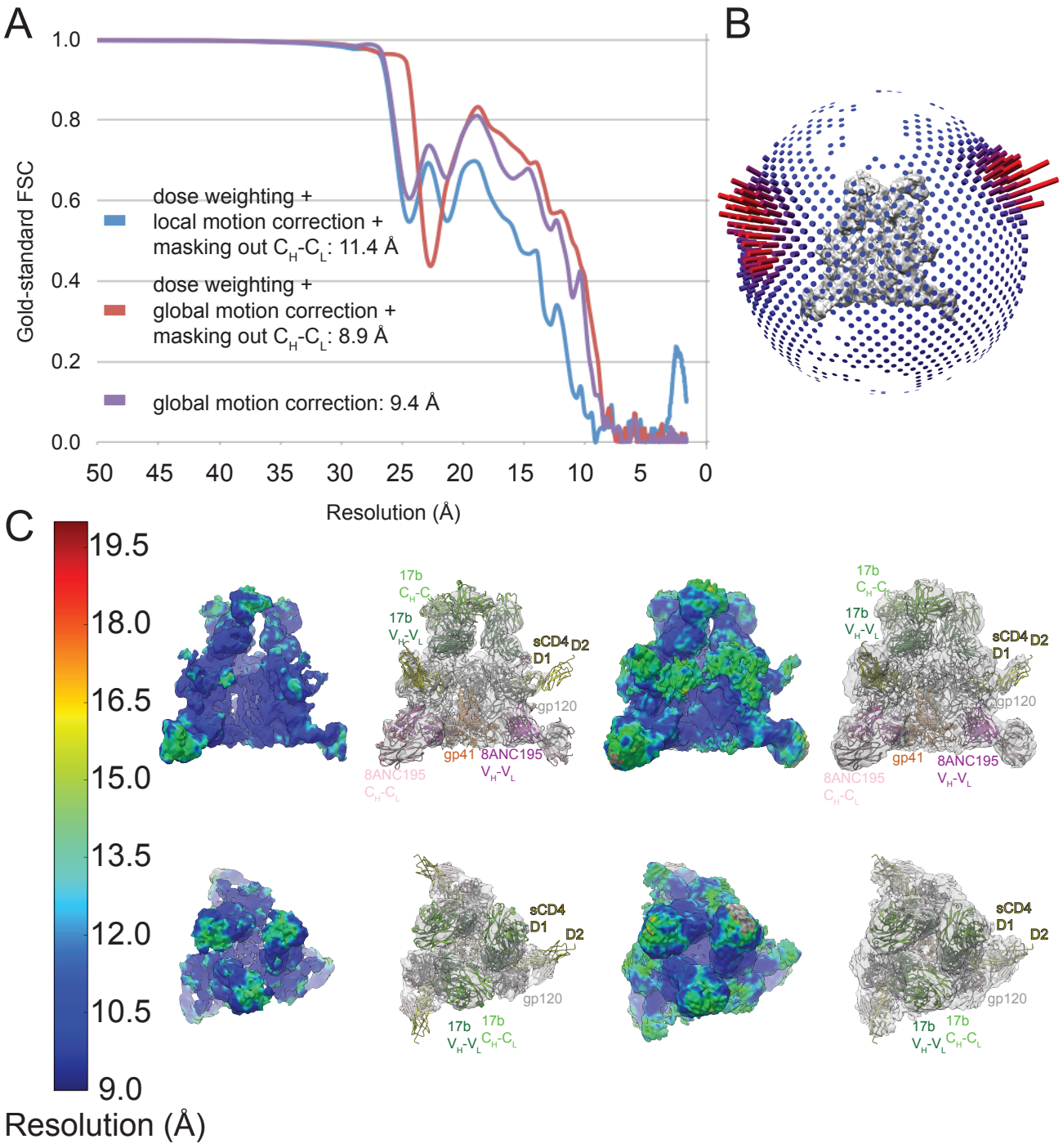

Fig. S2. EM structure analysis. (*A*) Gold-standard FSCs of reconstructions generated using different strategies. The 8.9 Å reconstruction was generated using dose weighting and masking out the Fab C_H-C_L domains. (*B*) Orientation distribution of the 8.9 Å reconstruction. (*C*) Local resolution estimation in the 8.9 Å reconstruction. The Env-sCD4-17b-8ANC complex is shown as side (top row) and top (bottom row) views. Local resolution estimations are shown for a high contour level (left) and a lower contour level (right) with fitted coordinates shown beside each. In the local resolution map, gray represents resolutions below 20 Å. The lower contour level was necessary to visualize density for the sCD4 D2 domain and V1V2 loop. These regions were estimated to be ~15 Å resolution.

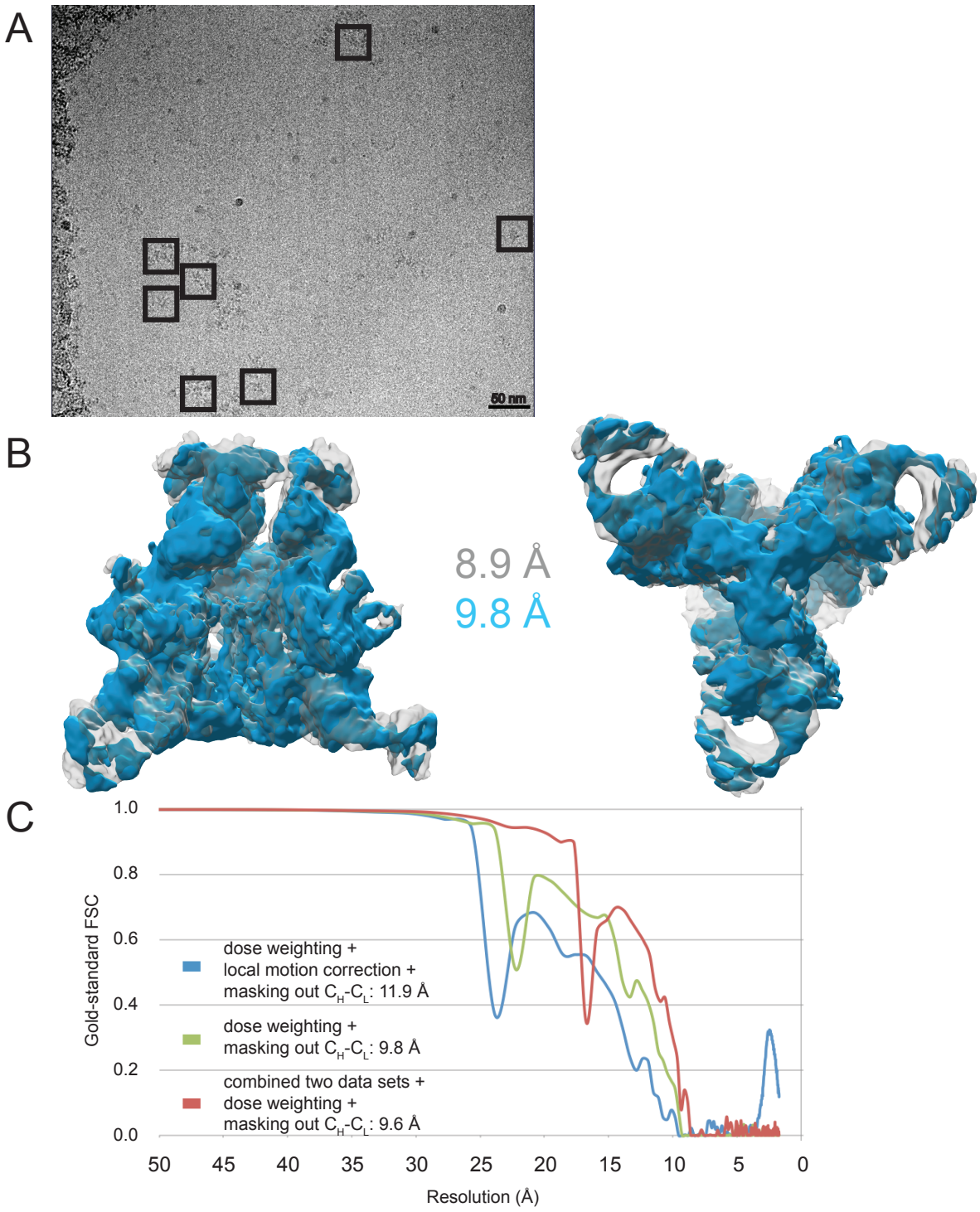

Fig. S3. Comparison of 8.9 Å and 9.8 Å Env-sCD4-17b-8ANC reconstructions. (*A*) Image of sample grid used for 9.8 Å reconstruction of the Env-sCD4-17b-8ANC complex. Examples of complex particles are boxed. The accumulated dose and defocus values were ~68 e-/Å^2 and ~3.3 µm defocus. (*B*) Superimposition of 8.9 Å and 9.8 Å reconstructions seen from the side (left) and bottom (right). (*C*) Gold-standard FSCs of reconstructions generated using different strategies. The 9.8 Å reconstruction was generated using dose weighting and masking out the Fab C_H-C_L domains. The calculated resolution was 9.6 Å when combining the two independent data sets (see Methods), using dose weighting, and masking out the Fab C_H-C_L domains.

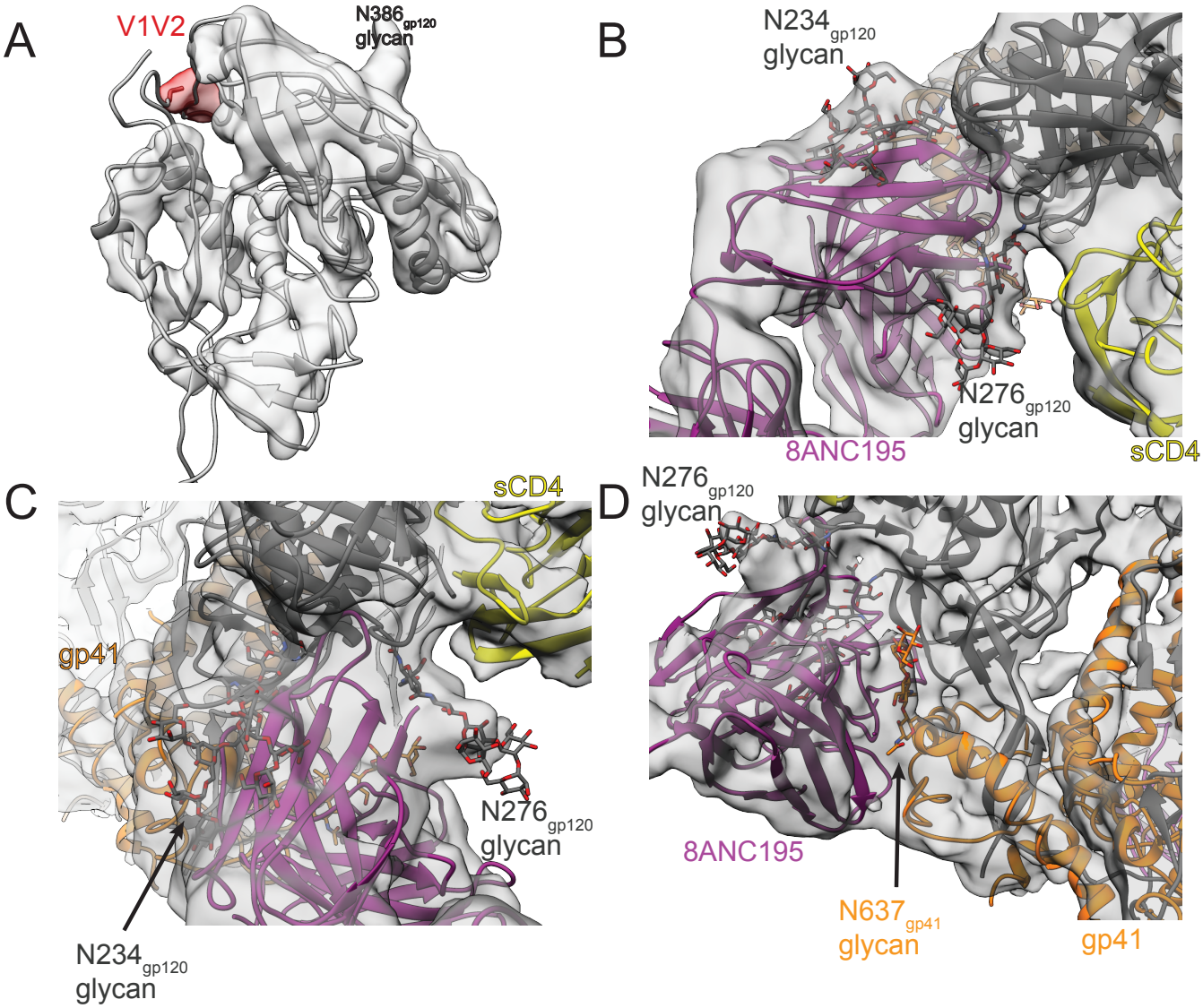

Fig. S4. Electron density in the 8.9 Å EM reconstruction. Close-up views of density in gp120 (*A*) and near the N-linked glycans attached to BG505 Asn234gp120 (*B*), BG505 Asn276gp120 (*C*), and BG505 Asn637gp41 (*D*). Glycans are shown as sticks.

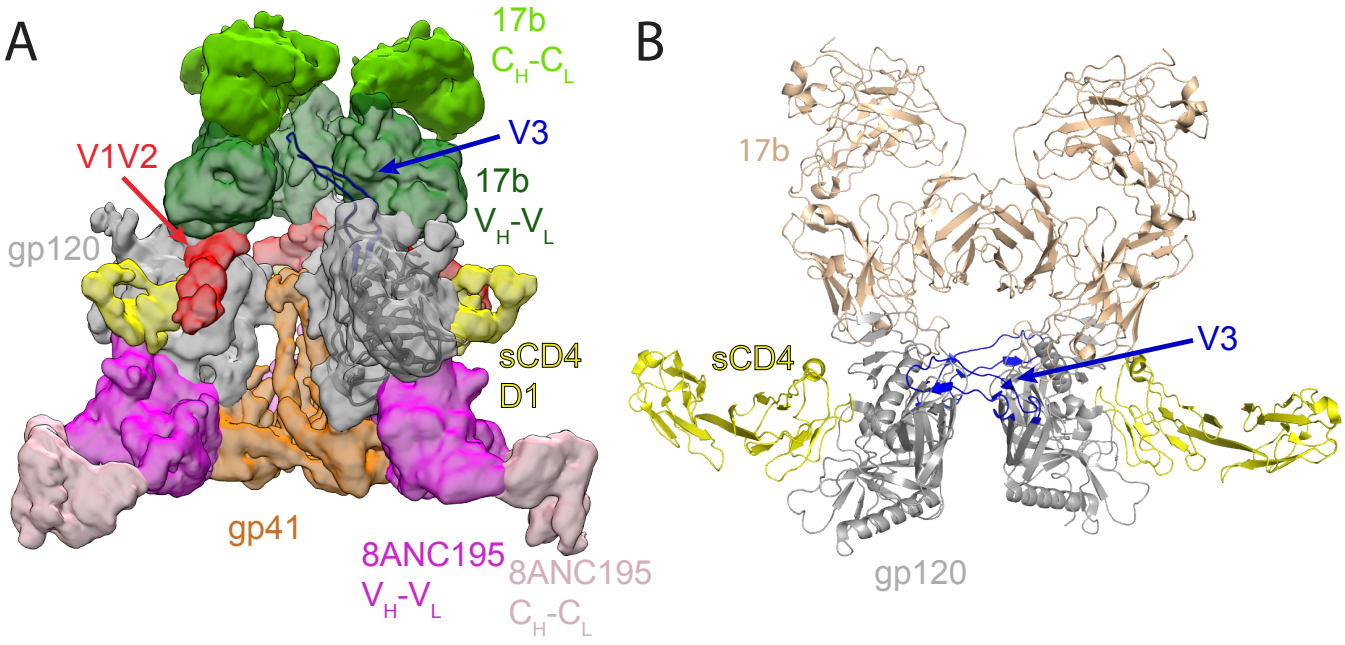

Fig. S5. V3 loop. (*A*) The gp120 V3 could not be localized in EM density of the sCD4-bound partially-open BG505 complex. The V3 loop position in the coordinates shown is derived from its position in a sCD4-bound gp120 core structure with an ordered V3 loop (34) (PDB 2QAD). (*B*) Crystal contacts in PDB 2QAD, a complex between a gp120 core (gray) with an ordered V3 loop (blue), sCD4 (yellow), and a CD4i Fab (wheat). The ordered V3 loops contact adjacent gp120s in the crystal.

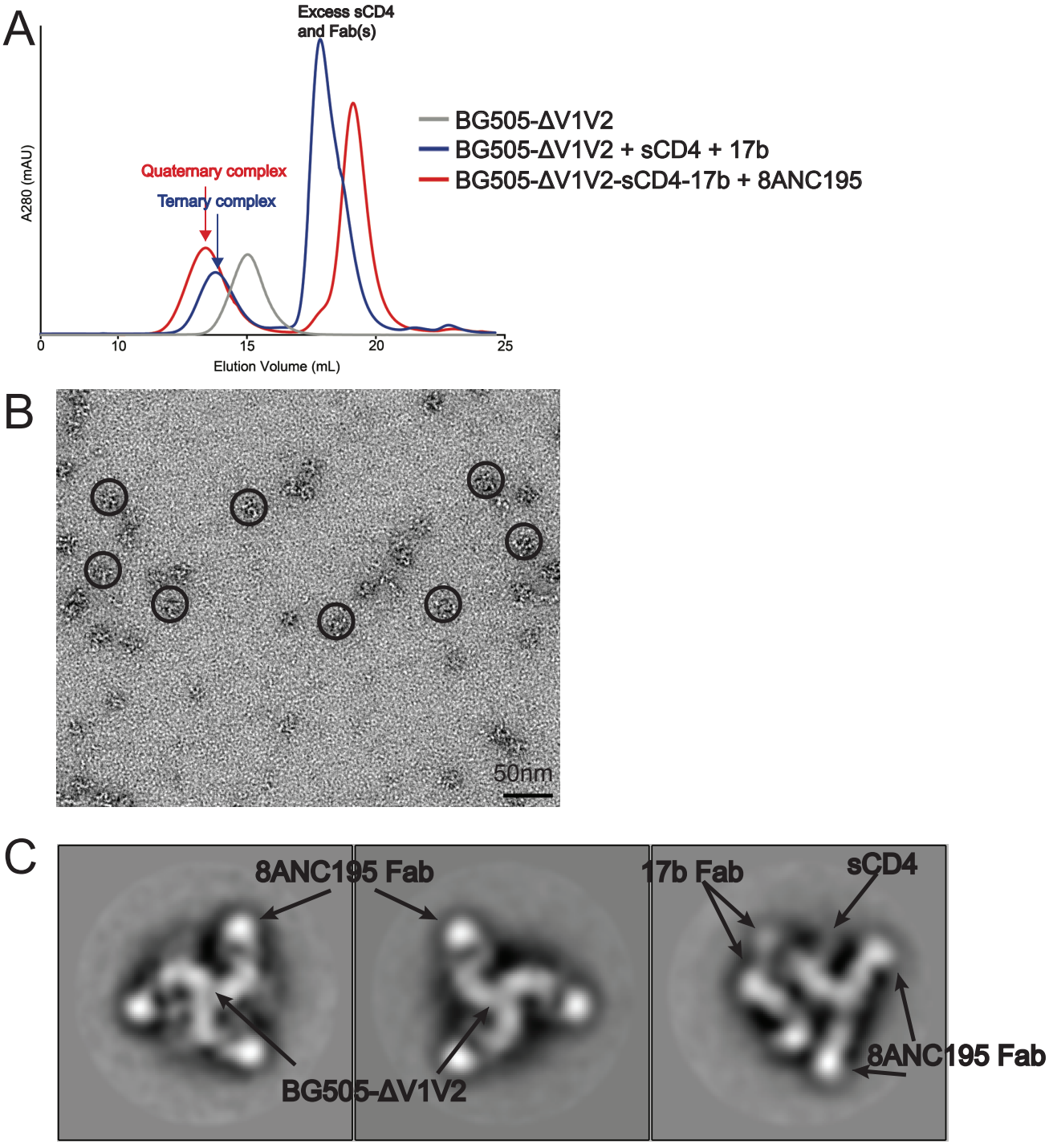

Fig. S6. Characterization of BG505-ΔV1V2. (*A*) Size exclusion chromatography (SEC) profiles showing SEC purification steps. The BG505-ΔV1V2-sCD4-17b ternary complex (blue) was purified first and then 8ANC195 Fab was added to form the quaternary complex (red). The faster-migrating peaks (12-15 mL) correspond to BG505-ΔV1V2 alone (gray), the ternary BG505-ΔV1V2-sCD4-17b complex (blue), and the BG505-ΔV1V2-sCD4-17b-8ANC195 complex (red). The slower migrating peaks (17-21 mL) correspond to free sCD4 and Fabs. (*B*) Image of the sample grid used for negative stain single particle reconstruction. Examples of complex particles are circled. (*C*) 2D class averages of the BG505-ΔV1V2-sCD4-17b-8ANC195 complex. Arrows point to identified ligands.